Colloid Polym Sci 274:928–937 (1996)

ORIGINAL CONTRIBUTION

T. Ogita
T. Sakabe
T. Yamada
H. Sano
H. Noguchi
C.Y. Xu
M. Matsuo

Morphology of poly(vinyl alcohol) gels assuring the greatest significant drawability

Received: 10 July 1995
Accepted: 8 March 1996

T. Ogita · T. Sakabe · T. Yamada
Department of Materials Science and Engineering
Faculty of Engineering
Yamagata University
Yonezawa 992, Japan

H. Sano · H. Noguchi
Fiber Research and Development Department
Technical Research Center
Kuraray Co. Ltd.
Kurashiki 710, Japan

C.Y. Xu · Prof. Dr. M. Matsuo (✉)
Department of Textile and Apprarel Science
Faculty of Human Life and Environment
Nara Women's University
Nara 630, Japan

Abstract Atactic poly(vinyl alcohol) (at-PVA) and syndiotactic poly(vinyl alcohol) (st. PVA) prepared by gelation/crystallization using dimethyl sulphoxide/water mixtures were drawn in a hot oven at 160 °C under nitrogen. The degrees of polymerization of at- and st-PVA were 2000 and 1980, respectively. The drawability of at- and st-PVA films was affected by the composition of the solvent mixture as well as by quenching temperature. The drawability of at- and st-PVA films prepared by using the solvent mixture containing 60% of dimethyl sulphoxide and 40% of water became more pronounced as the temperature of gelation/crystallization decreased and the draw ratio reached maximum value at −80 °C. Namely, the greatest significant drawability was the same condition for at- and st-PVA films in spite of the different stereo-regularity. Even in this common best condition for significant drawability, however, the morphological properties of swollen gels and of the resultant dry gel films are different each other, dependent upon the tacticity. For at-PVA, small-angle light scattering under Hv polarization condition could not be observed in the swollen gels and in the dry films when the solutions were quenched at temperatures < -10 °C. In contrast, for st-PVA, the X-type scattering pattern from swollen gels became clearer as the temperature decreased but the pattern became indistinct under drying process at ambient condition. On the other hand, the fibrillar textures within the at- and st-PVA dry films became finer and the orresponding crystallinity became lower as the temperature of gelation/crystallization decreased. Thus it turned out that the morphological properties of the swollen gels and of the dried films play an important role to assure the greatest significant drawability.

Key words Atactic poly(vinyl alcohol) – syndiotactic poly(vinyl alcohol) – gelation/crystallization – dimethyl sulphoxide/water mixtures – small-angle light scattering

Introduction

The range of application of polyethylene is limited by its low melting point. To improve heat-resistance, cross-linking of polyethylene has been performed with γ- and electron-beam irradiations [1–3]. Most irradiation studies, however, have dealt with undrawn films. Recently, the application of cross-linking to an oriented system has been carried out by Pennings et al. by using dicumyl

peroxide to cross-link as-spun ultrahigh molecular weight polyethylene films [4]. Based on their concept, Matsuo and Sawatari have tried to introduce dicumyl peroxide into ultrahigh-molecular-weight polyethylene gel films prepared by gelation/crystallization from solution in decalin and after evaporating the solvent, dry gel films could be readily elongated up to 100 times at 150 °C under nitrogen [5, 6]. Surprisingly, the values of storage modulus were 114 GPa at 20 °C and 2.0 GPa at 200 °C, respectively. Unfortunately, drastic decrease in the storage modulus was observed around 150 °C due to the melting of crystallites independent of cross-linking. Thus, poly(vinyl alcohol) (PVA) is one of the important flexible polymers to produce high-modulus and high-strength fibers, since PVA has heat-resistant property because of a number of hydrogen bonds and the decrease in storage modulus with increasing temperature beyond 150 °C is not considerable. Therefore, ultradrawing of PVA films has been extensively investigated and good results have been reported [7–12].

In previous paper [10], the drawability of atactic poly(vinyl alcohol) (at-PVA) has been studied as a function of degree of polymerization, composition of mixed solvent, concentration of solution, and the temperature of gelation/crystallization. The samples of PVA with degree of polymerization of 2000 and 4000 and with a degree of hydrolysis of 98 mol% were used. The composition of dimetyl sulphoxide (Me_2SO) and water mixture, Me_2SO/H_2O chosen were 100/0, 70/30, and 50/50. The solutions were prepared by heating the well-blended polymer/solvent mixture at 105 °C for 40 min and the homogenized solution was poured into an alminum tray or a Petri dish which was placed into a cold bath set at the desired temperature in the range of $-50 \sim 100$ °C for 24 h, thus generating a gel. The gel was vacuum-dried to evaporate the solvent at chosen temperatures. Through a series of experiments, it was found that the maximum draw ratio of dry gel films could be realized when the gel was prepared from a solution with 70/30 composition by quenching at − 50 °C. Although this conclusion was certainly important to know the outline of optimum condition assuring the greatest significant drawability, the experimental results were too few to derive a definite conclusion. To facilitate understanding of the optimum condition assuring the greatest significant drawability, this paper deals with the more detailed experiments in terms of morphological aspect using solvents with various Me_2SO/H_2O compositions. Furthermore, the same treatments were done for syndiotactic PVA (st-PVA) gels to understand the optimum condition in relation to the difference of tacticity.

Experimental section

Sample preparation

Two kinds of PVA specimens were used in the present work.

1) The samples of at-PVA powder used has a degree of polymerization of 2000 and a degree of hydrolysis of 98%. The Me_2SO/H_2O compositions chosen as solvent were 100/0, 90/10, 80/20, 70/30, 60/40, 50/50, 40/60, 30/70, 20/80, 10/90, and 0/100. The solutions with concentration of 10 vol% were prepared by heating the well-blended polymer/solvent mixture at 105 °C for 40 min under nitrogen. The homogenized solution was poured into a Petri dish which was placed into a bath set at 105 °C. After then the Petri dish was placed in a refrigerator at the desired temperature in the range of $-80 \sim 20$ °C for 24 h, thus generating a gel. The gel was maintained without evaporating the solvent more than 10 days at 20 °C. In this stored period, the shrinkage of gels occurred drastically at initial stage and tended to level off. After then, the gels were immersed in a water bath at 5 °C for 1 week to remove Me_2SO. Through these stored processes, the gels kept good dimensional stability after drastic shrinkage. The fresh gel films were dried with a fixed dimension by a circular ring under ambient condition and then the resultant dry gels were vacuum-dried for 1 day to remove residual traces of solvent. Without the immersion treatment, the fresh gel films were broken in the drying process because of the drastic shrinkage. The dry gel films were cut into strips of length 30 mm and width 10 mm. The strip was clamped in a manual stretching device in such a way that the length to be drawn was 20 mm. The specimen was placed for 5 min under nitrogen at 160 °C and elongated manually to the maximum draw ratio. Immediately after stretching, the stretcher with the sample was quenched to room temperature. This is the best condition to assure significant drawability without carbonization.

2) The sample used was st-PVA pellets with a 99.4% degree of hydrolysis and with a syndiotactic diad content of 61.2%. The degree of polymerization was 1980 estimated from viscosity. Based on the pretreatment experiments for drawability of at-PVA, the Me_2SO/H_2O compositions chosen as solvent were determined to be 70/30 and 60/40. The preparation of st-PVA gel by quenching solutions with the concentration of 10 vol% was quite similar to that of at-PVA gel. The elongation was done in the same manner as in the case of at-PVA.

Colloid & Polymer Science, Vol. 274, No. 10 (1996)

Table 1 Birefringence, Young's modulus, and tensile strength at maximum draw ratio, λ_{max}, of at-PVA films prepared by quenching the solutions with the indicated compositions of mixed solvent at temperatures, 20, −10, −40, and −80 °C

Quenching temperature (°C)	Me_2SO/H_2O composition (vol%)	Maximum draw ratio λ_{max}	Birefringence ($\Delta \times 10^3$)	Young's modulus (GPa)	Tensile strength (GPa)
	40/60	10.1	35.5	25.6	0.47
	50/50	10.7	36.2	26.8	0.57
20	60/40	11.4	36.8	27.3	0.62
	70/30	11.2	36.6	27.0	0.63
	80/20	–	–	–	–
	40/60	10.3	38.5	27.3	0.52
	50/50	11.3	38.8	30.8	0.62
−10	60/40	11.5	40.3	32.3	0.70
	70/30	11.4	39.4	31.5	0.67
	80/20	10.3	36.9	31.3	0.60
	40/60	10.7	38.8	28.5	0.66
	50/50	12.0	39.4	31.3	0.73
−40	60/40	12.7	40.5	32.9	0.78
	70/30	12.5	39.8	31.9	0.69
	80/20	10.8	37.4	31.8	0.63
	40/60	11.1	39.2	29.2	0.73
	50/50	12.8	40.3	32.2	0.79
−80	60/40	13.8	40.7	34.5	0.84
	70/30	13.5	40.5	33.5	0.74
	80/20	12.7	39.7	32.1	0.65

Sample characterization

The number-average degree of polymerization of at- and st-PVA described before were determined from G.P.C. measurements of a 0.25 wt % tetrahydrofuran solution of poly(vinyl acetate) which was obtained by acetylation of the corresponding parent PVA by using the equation of Mori [13].

The density of the films was measured by pycnometry in a medium of *p*-xylene and carbon tetrachloride. Before the measurements were made, the specimen was cut into fragments and vacuum-dried for 1 day. The crystallinities of at- and st-PVA films were calculated by using the intrinsic densities of crystalline and amorphous phases to be 1.345 and 1.269, respectively [1, 4], on the basis of the assumption that the intrinsic densities are constant, independent of elongation. The density measurements were carried out several times to check the reproducibility of the values, since the difference in density between crystalline and amorphous phases is not large.

Here, we must emphasize the difficulty in determining a maximum draw ratio exactly. For this purpose, as an example, we shall explain briefly the present treatment for the specimen with maximum draw ratio, λ_{max}, of 10.1 which was listed as the value of the crystallinity of specimens prepared by quenching at-PVA solution with 40/60 composition at 20 °C in Table 1 (see later). Actually, it was very difficult to judge whether the draw ratio is 10.1 by a ruler. Accordingly, by a ruler microscopy, we measured again the draw ratios for several specimens whose draw ratio had been determined to be 10.1 by a ruler. In this case, the draw ratios were in the range $10.0 \sim 10.2$. Therefore, the average value of the crystallinities of a number of specimens with $\lambda_{max} = 10.1$ was listed in Table 1 (see later).

Young's modulus and tensile strength of the specimens were measured with a tensile tester at room temperature. The drawn specimen was cut into strip of a length of 60 mm and with the width of 1.5 mm and the strip was clamped over a length of 10 mm at the end.

Small-angle light scattering (SALS) under Hv polarization condition was observed with a 15 mW He-Ne gas laser as a light source. The scattered intensity from gels was too weak to detect by photographic film, since most of beam could not pass through the analyzer. Therefore, the reflected pattern on the gel surface was detected by commercial camera.

The measurements for x-ray diffraction and birefringence were discussed elsewhere in detail [10].

Results and discussion

Figure 1 shows the condition of gel formation and the appearance of light scattering patterns under Hv polarization condition. The scattering shows X-type patterns indicating the existence of anisotropic rods (fibrils), the optical axes being oriented parallel or perpendicular to the rod axis. The preparation of gels was tried in the wide ranges of the Me_2SO/H_2O compositions and of temperatures of gelation/crystallization, T_{gel}. It was found that

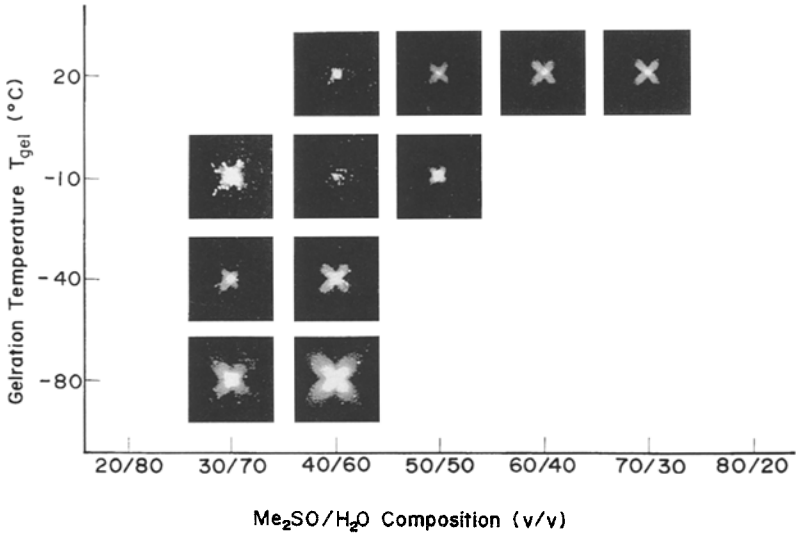

Fig. 1 Hv light scattering patterns of the at-PVA swollen gels prepared from the solutions with indicated Me_2SO/H_2O compositions at the indicated gelation temperatures, T_{gel}

the gelation becomes more pronounced as the quenching temperature of solution becomes lower. But gelation did not occur at lower and higher contents of Me_2SO ($Me_2SO \geq 90$ and ≤ 20) even at temperatures lower than 0 °C. Hence it should be noted that even in the range of Me_2SO/H_2O compositions where gelation/crystallization occurred, the appearance of Hv pattern is limited as shown in Fig. 1. For the gel prepared from solutions with 40/60 composition, the patterns were observed in the given temperature range, $-80 \sim 20$ °C, and they became distinct with decreasing temperature. Furthermore, at the 30/70 composition, the gelation/crystallization did not occur at 20 °C but the swollen gels prepared at temperatures ≤ -10 °C provided X-type pattern and the pattern became clearer as gelation/crystallization temperature, T_{gel}, became lower. In contrast, the patterns for 60/40 and 70/30 compositions could not be observed at temperatures ≤ -10 °C, indicating the existence of rods with no optical anisotropy. According to the previous work [10], the maximum drawability was assured, when the solution with 70/30 composition was quenched at temperature ≤ -50 °C. This indicates that when gel consists of rod-like (fibrous) texture with no optical anisotropy it assures the greatest significant drawability. If this is the case, it is evident that the drawability of at-PVA gels surely depends on whether anisotropic rod-like textures within swollen gels exist or not. To check such an interesting concept, the following experiments were carried out in terms of morphology and mechanical aspects in detail.

Figure 2 shows the change in weight of at-PVA specimens which were prepared by gelation/crystallization at

Fig. 2 Change in weight of the at-PVA swollen gels during the storage period at 20 °C. The gels were prepared from the solutions with Me_2SO/H_2O compositions, (a) 40/60, (b) 50/50, (c) 60/40, and (d) 70/30 at the gelation temperatures, T_{gel}, ○ 20, ◑ −10, ◐ −40, and ● −80 °C, respectively

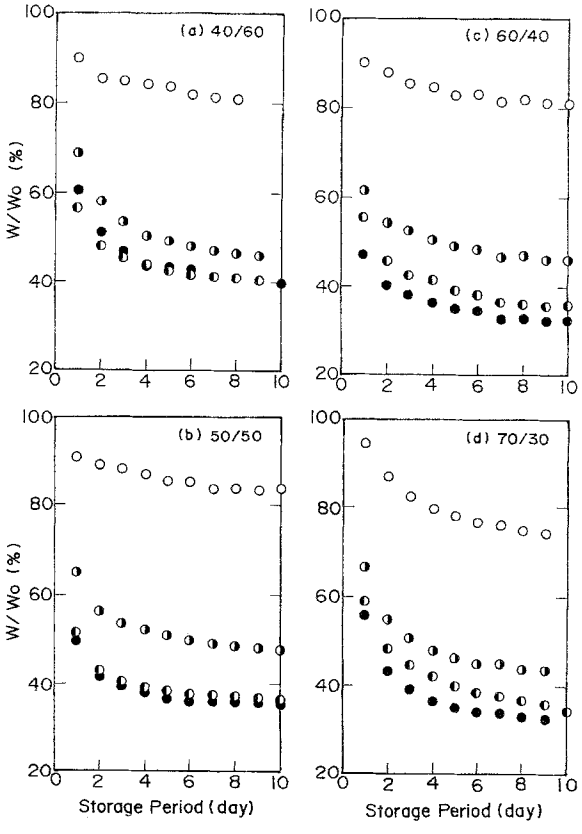

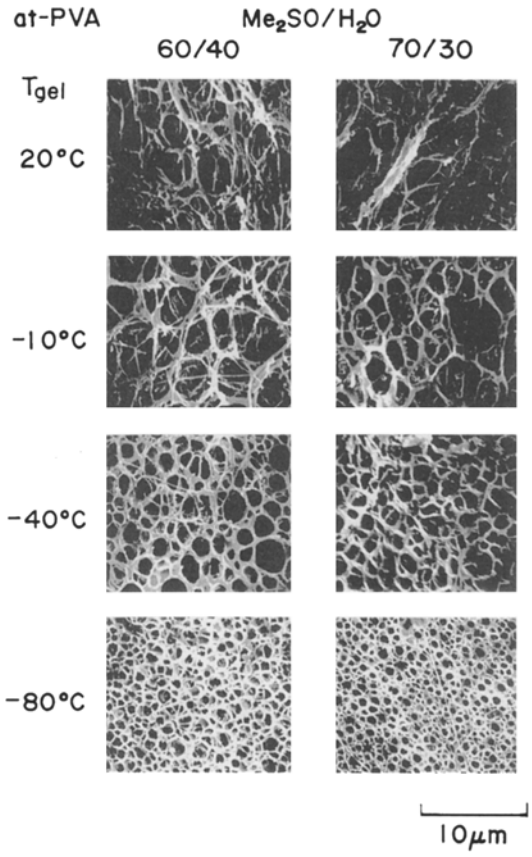

Fig. 3 Scanning electron micrographs of the at-PVA undrawn films prepared by gelation at the indicated temperatures

various temperatures and were stored at 20 °C for the indicated days. The change in the weight is attributed to the flow of solvent by the shrinkage of gel which is so-called syneresis. The degree of shrinkage is defined as W/W_0, where W_0 and W are the weights of just prepared gels and the weight of stored gels measured after day by day, respectively. The degree of shrinkage became more pronounced as the temperature of gelation/crystallization, T_{gel}, became lower. This tendency was slightly significant for the gels prepared from solutions with 60/40 and 70/30 assuring the greatest significant drawability. It may be expected that such drastic shrinkage at lower temperature is attributed to the morphology of the resultant dried gel films. In seeking a clear answer to the expectation, the morphology of the dried gel films was observed with scanning electron microscopy (SEM).

Figure 3 shows the change in the appearance of undrawn dry gel fims prepared by evaporating solvent from swollen gels prepared by quenching solutions with 60/40 and 70/30 compositions of mixed solvents. The texture is apparently meshy fibrillar-like interconnected lamellar crystals. With decreasing the gelation/crystallization temperature, T_{gel}, the fibrillar texture becomes finer. Similar tendency was confirmed for the solutions with another compositions but not so drastic in comparison with the change in Fig. 3. Wide-angle x-ray diffraction (WAXD) pattern (end view) suggested a slight uniplanar orientation of the (1 0 1) plane parallel to the film surface, probably due to the small planar tension during gelation as described in the previous paper [10]. The uniplanar orientational degree was more pronounced as the gelation/crystallization temperature, T_{gel}, became lower. The reflection of the (1 0 1) plane indicates that meshy fibrous textures observed with SEM are oriented randomly on the film surface. As discussed later, the Hv scattering pattern (for example, see $\lambda = 1$ in Fig. 8) from dried gel films prepared by gelation/crystallization temperatures ≤ 20 °C displays indistinct circular pattern. Such a circular pattern is due to the scattering from a system composed of a random array of crystallites that are compared smaller with the wavelength of incident beam. This indicates that fine fibrous textures in Fig. 3 show no optical anisotropy. If fibrous textures performed in the swollen gels are preserved in the dry process, as shown in Fig. 3, an increase in the degree of shrinkage with decreasing temperature is attributed to the formation of fine fibrous structures with no optical anisotropy.

Table 1 summarizes birefringence, Young's modulus, and tensile strength at the maximum draw ratio, λ_{max}, for the dried gel films which were prepared from solutions with different Me_2SO/H_2O compositions by quenching the solutions at the indicated temperatures. Each value listed in Table 1 was selected as an average value from the experimental results measured for a number of same kinds of test specimens. The maximum draw ratio could be realized by the elongation of the dried gel film prepared by quenching the solution with 60/40 composition at -80 °C. The films with the maximum draw ratio also gave the maximum values of birefringence, Young's modulus, and tensile strength. In contrast, for the gels with 40/60 composition showing X-type pattern in the given gelation/crystallization temperature range, the maximum draw ratio of the resultant dry films is less sensitive to the decrease in gelation temperature in comparison with the temperature dependence of maximum draw ratios of the films with 70/30 and 60/40, and consequently increases in the corresponding Young's modulus and tensile strength with decreasing the temperature are not significant. Hence, it is of interest to consider the relationship between the drawability and the existence of anisotropic rod-like textures.

A series of experimental results indicates that the facile drawability can be realized in the case where continuous uniform fine fibrous (rod-like) texture with no optical anisotropy were performed within the dried films. If this is

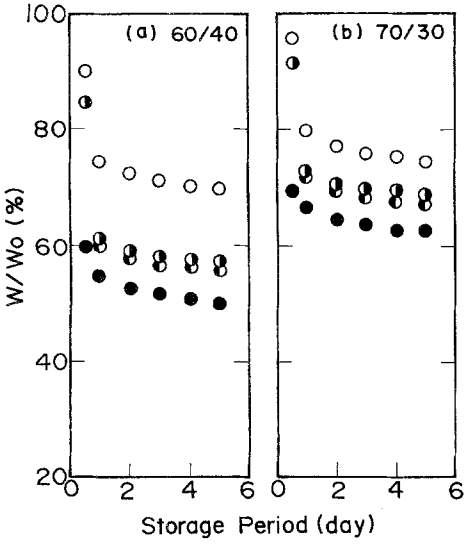

Fig. 4 Change in weight of the st-PVA swollen gels during the storage period at 20 °C. The gels were prepared from the solutions with Me_2SO/H_2O compositions, (a) 60/40 and (b) 70/30 at the gelation temperatures, T_{gel}, ○ 20, ◑ −10, ◐ −40, and ● −80 °C, respectively

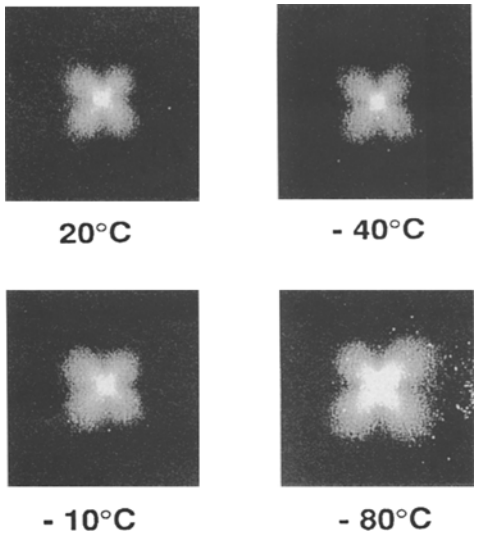

Fig. 5 Hv light scattering patterns from the st-PVA swollen gels prepared from solutions with 60/40 composition at the indicated gelation temperatures, T_{gel}

the case, it is evident that the uniform fine structure plays an important role to transmit the inner tension smoothly under elongation process.

To give generality to this concept, the same experiment was carried out for st-PVA. Unfortunately, the amount of st-PVA furnished was very small to carry out detail experiments and main experiments were limited to the two compositions, 70/30 and 60/40.

Figure 4 shows the change in weight of swollen st-PVA gels which were prepared by quenching solutions with 60/40 and 70/30 compositions at various temperatures and were stored at 20 °C for the indicated days. The degree of shrinkage was not so sensitive to the gelation/crystallization temperature, T_{gel}, in comparison with that at-PVA, except for the specimen prepared by gelation/crystallization at 20 °C. Especially for the 70/30 composition, the degree of shrinkage of st-PVA was much lower than that of at-PVA ones, independent of gelation/crystallization temperature, T_{gel}. The shrinkage for all the gels tended to level off after 5 days.

Figure 5 shows X-type Hv light scattering patterns from swollen gels prepared from the solutions with 60/40 composition at the indicated temperatures. This phenomenon is quite different from the result for at-PVA gels showing in Fig. 1. Of course, the patterns are one of examples and the similar patterns could be observed for every gel prepared by quenching solutions with 30/70 ~80/20 compositions. This means that the stereo-regularity plays an important role to form anisotropic rod-like

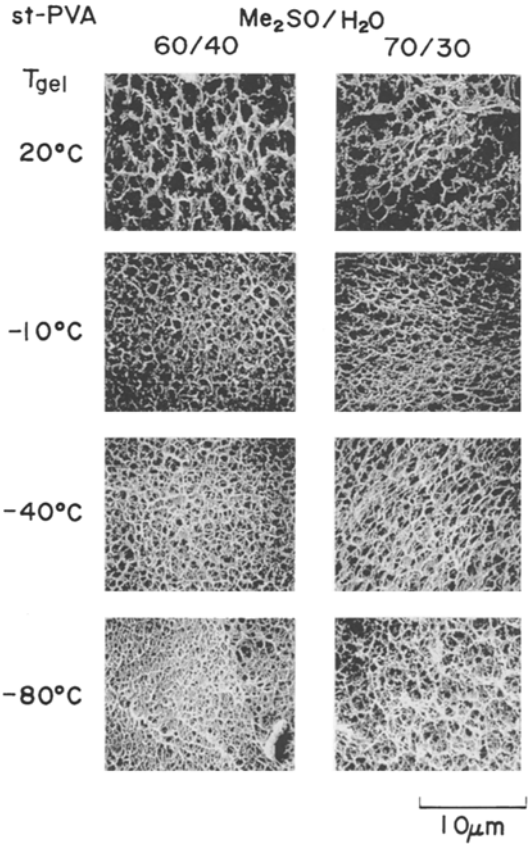

Fig. 6 Scanning electron micrographs of the st-PVA undrawn films prepared by gelation at the indicated temperatures, T_{gel}

Colloid & Polymer Science, Vol. 274, No. 10 (1996)

Table 2 Crystallinity, birefringence, Young's modulus, and tensile strength at maximum draw ratio, λ_{max}, of st- and at-PVA films prepared by quenching the solutions with 60/40 and 70/30 compositions of mixed solvent at temperatures, 20 °, −10 °, −40 °, and −80 °C

Quenching temperature (°C)	Me_2SO/H_2O composition (vol%)	Maximum draw ratio λ_{max}	Crystallinity (%)	Birefringence ($\Delta \times 10^3$)	Young's modulus (GPa)	Tensile strength (GPa)
st-PVA						
20	60/40	10.0	33.5	30.5	22.1	0.31
	70/30	10.2	33.5	23.3	17.5	0.22
−10	60/40	11.0	34.2	31.5	25.0	0.42
	70/30	11.2	35.0	29.5	25.3	0.28
−40	60/40	11.3	35.1	31.5	25.3	0.52
	70/30	11.4	35.4	31.0	25.8	0.40
−80	60/40	11.8	35.1	34.0	28.1	0.70
	70/30	12.1	35.6	33.8	26.6	0.47
at-PVA						
20	60/40	11.4	32.9	36.8	27.3	0.62
	70/30	11.2	33.2	36.6	27.0	0.63
−10	60/40	11.5	34.0	40.3	32.3	0.70
	70/30	11.4	34.5	39.4	31.5	0.67
−40	60/40	12.7	34.4	40.5	32.9	0.78
	70/30	12.5	35.1	39.8	31.9	0.69
−80	60/40	13.8	34.6	40.7	34.5	0.84
	70/30	13.5	35.1	40.5	33.5	0.74

textures, being more or less regular aggregation of crystallites, within the swollen gels.

Figure 6 shows the change in the appearance of undrawn gel films under SEM. It is seen that at temperatures ≤ -10 °C, the meshy fibrillar texture became much finer in comparison with at-PVA. In spite of finer structures of st-PVA, the syneresis of st-PVA gels as shown in Fig. 4 is not considerable than that of at-PVA gels. A question arises as to why the degree of shrinkage of st-PVA gels is lower than that of at-PVA ones (see Fig. 4) in spite of the formation of anisotropic rod-like (fibrous) textures at lower gelation/crystallization temperature, T_{gel}, observed by Hv polarization condition (see Fig. 5). This phenomenon is in contradiction with that confirmed for at-PVA. This reason still remains an unsolved problem. However, it is evident that fibrous textures in the at-PVA swollen gels are uniform rod-like textures with no optical anisotropy and the formation of uniform structure under the progression of gelation causes significant effect on throwing out solvent.

Table 2 lists birefringence, Young's modulus, the tensile strength at the maximum draw ratios λ_{max} of the st-PVA and at-PVA dried gel films prepared from solutions with 60/40 and 70/30 compositions by quenching the solutions at the indicated gelation/crystallization temperatures. The measurements were repeated more than eight times for the same kinds of test specimens. To facilitate understanding of the drawability between st- and at-PVA films, the same data of at-PVA films with 60/40 and 70/30 compositions were listed again in Table 2. The maximum draw ratios for each condition are a little bit lower than the corresponding maximum values of at-PVA. Obviously, the draw ratio is sensitive to the temperature of gelation/crystallization. The crystallinity increased, as gelation/crystallization temperature decreased. At each temperature, the crystallinity of st-PVA dried gel film become a little bit higher than that of at-PVA. This is probably thought to be due to better stereo-regularity of st-PVA which hampers the facile drawability.

Birefringence depends on the maximum draw ratio of each specimen prepared by the indicated conditions. The value increases with decreasing the gelation/crystallization temperature, T_{gel}, but the value of st-PVA film is lower than that of at-PVA. Such higher molecular orientation of at-PVA films is obviously attributed to the higher draw ratio of at-PVA films.

Young's modulus and the tensile strength depend on the draw ratio. In addition to draw ratio, the values of Young's modulus and tensile strength become higher, as the gelation/crystallization temperature, T_{gel}, decreases. The values of at-PVA films are higher than those of st-PVA films. This indicates that the Young's modulus and the tensile strength of drawn PVA films are more sensitive to the molecular orientational degree associated with birefringence than crystallinity. Namely, the maximum values of crystallinity at each maximum draw ratio of films prepared by the indicated conditions, are in the range $33 \sim 36\%$, but the crystallinities of the films with each maximum draw ratio, slightly increases with decreasing the temperature of gelation/crystallization.

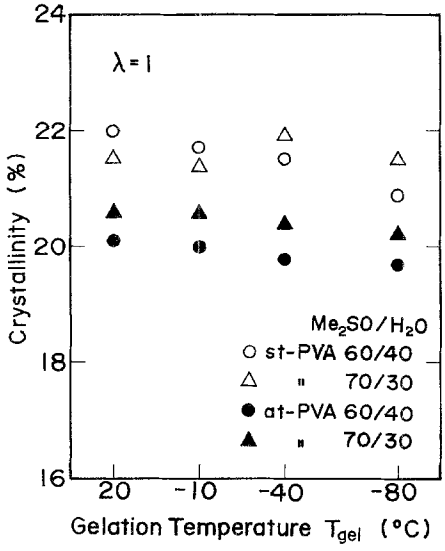

Fig. 7 Crystallinity of undrawn st-PVA and at-PVA prepared from the solutions with the indicated compositions at the gelation temperatures, T_{gel}

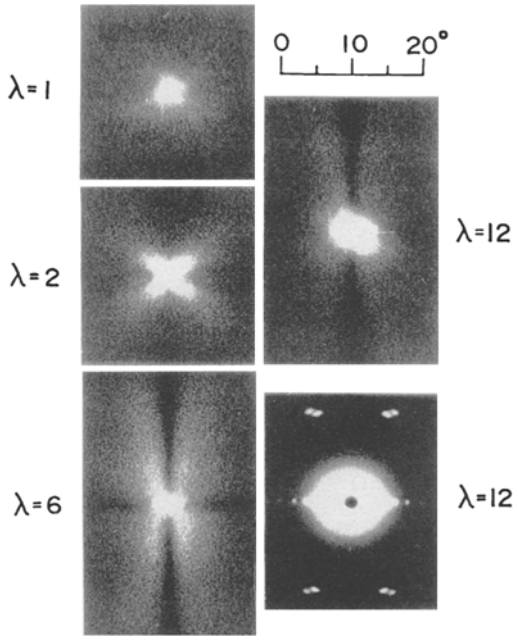

Fig. 8 Changing in Hv light scattering patterns observed for the at-PVA films prepared by gelation/crystallization of solutions with 60/40 composition at $-40\,^{\circ}C$ and the WAXD patterns at $\lambda = 12$

Figure 7 shows the crystallinity of undrawn st- and at-PVA films prepared by the indicated conditions. The crystallinity tends to be lower with decreasing the temperature of gelation/crystallization, T_{gel}, for all the compositions. Interestingly, facile drawability could be realized by elongation of original (undrawn) films with the lowest crystallinity in spite of the small difference, although the crystallinity of the corresponding drawn films became highest. The same tendency was already confirmed for at-PVA films with P = 4000 [10].

This can be rationalized by assuming that the solvent with 60/40 composition is a good solvent for at-PVA and st-PVA. Especially, the specific viscosity η_{sp} of at-PVA solution with 60/40 composition measured at 100 °C, was highest among all the solutions with different compositions and the value was much higher than the highest value of st-PVA solution obtained at 60/40 composition. This indicates that the size or spatial extension of at-PVA molecules become greatest in the solution with 60/40 composition. Judging from the highest specific viscosity of at-PVA solutions with the 60/40 composition, it may be expected that intermolecular entanglement in solution and gelation at such low temperature as $-80\,^{\circ}C$ hamper crystallization and promote the formation of fine uniform fibrous textures with no optical anisotropy. Such a gelation/crystallization mechanism is quite different from that of polyethylene [15–17].

The difference may be explained from the unusual change of Hv light scattering patterns from at-PVA films showing development of an unusual clear X-type pattern and a normal WAXD pattern exhibiting small angular spread of the strong reflections at $\lambda = 12$ as shown in Fig. 8. The results were obtained from at-PVA dry gel films prepared by gelation/crystallization at $-40\,^{\circ}C$. Incidentally, the patterns observed at temperatures $\leq -10\,^{\circ}C$ were confirmed to be almost the same as those in Fig. 8.

As shown in Fig. 8, the Hv scattering from dry gel film at an undrawn state ($\lambda = 1$) displays an indistinct circular pattern indicating the scattering from a system composed of a random array of crystallites smaller than the wavelength of incident beam. Elongation up to $\lambda = 2$ causes development of a clear X-type pattern whose lobes are extended in the horizontal direction exhibiting the preferential orientation of rods in the stretching direction. Further elongation beyond $\lambda = 6$, however, gives X-type pattern whose lobes are extended in the meridional direction. Namely, the Hv scattering lobes changed from the horizontal to the meridional direction. In the viewpoint of the theory of SALS under Hv polarization, such lobes extended to the meridional direction must be interpreted as a contribution of scattering from rods with extremely high orientation perpendicular to the stretching direction. Such an unusual change of lobes has been also observed at initial draw ratio ($\lambda \leq 4$) of poly(ethylene terephthalate) [18] and poly(tetramethylene terephthalate) films, associated with the oriented crystallization [19]. A WAXD pattern at $\lambda = 12$ exhibits small spreads of the strong reflections from each crystal plane, indicating a high degree of orientation of the b-axis (fiber axis) with respect to

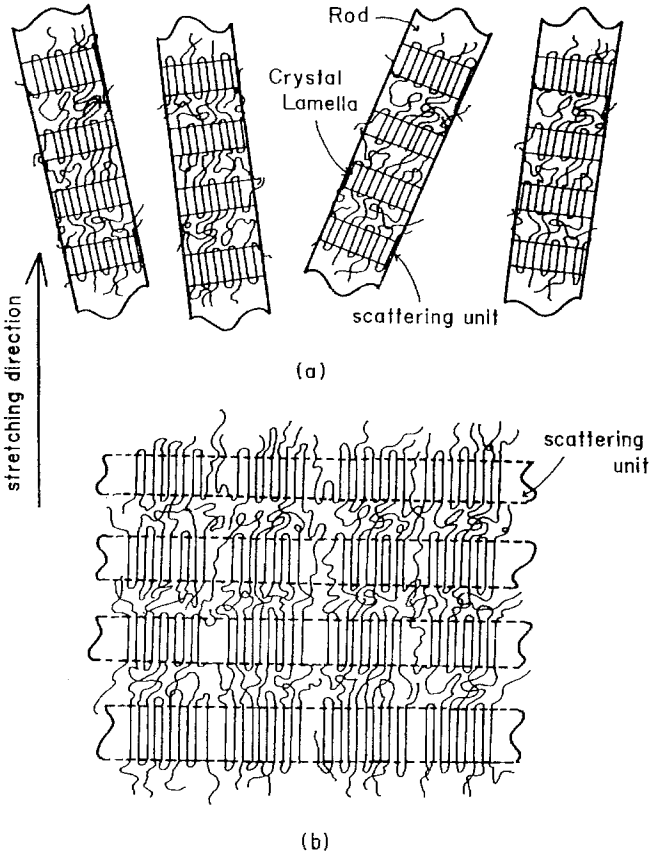

Fig. 9 Model proposed to explain change in Hv light scattering patterns in Fig. 8

the stretching direction. The spread became sharper with increasing draw ratio and any unusual change of WAXD pattern could not be observed at any draw ratio.

In order to explain the adequacy of Hv patterns in Fig. 8 the same schematic diagrams as has been presented already [10], are proposed again as Fig. 9 in the present work, in which (a) shows the orientation of rods at initial draw ratio and (b), the orientation at draw ratio $\lambda > 6$. In model (a), rods are oriented predominantly with respect to the stretching direction and the crystallites within a rod are connected to each other and the crystal axis, corresponding to the optical axis, is oriented predominantly parallel to the stretching direction. Model (b) is significant to explain the drastic change of Hv scattering lobes from the horizontal to the meridional direction. As shown in model (b), a scattering unit corresponds to a new rod-like structure that is formed by a lateral coalescence of rods during further elongation beyond $\lambda > 6$. The models (a) and (b) are consistent with the drastic change of the profile of the patterns without considering any unusual orientation of rods. As discussed already elsewhere [10], the existence of the crystal lamellae within the drawn film must be confirmed by small-angle x-ray measurements. However, a scattering maximum in the meridional direction was too indistinct to show the pattern here. This is probably due to the fact that the difference of electron density between crystal amorphous phases is too small to give a distinct scattering maximum. Incidentally, the first order scattering maximum in the meridional direction was confirmed already for the films which were obtained by drying of swollen gels at 20 °C prepared by gelation/crystallization from solution with 70/30 composition at −50 °C [10].

Hv light scattering patterns similar to Fig. 8 have been also observed for the elongation process of st-PVA dry gel films. The difference was confirmed to be very small. That is, the scattering patterns from undrawn st-PVA films show indistinct duller X-type. However, essential difference between at- and st-PVA films could not be observed at each draw ratio. WAXD patterns exhibited the same profile showing small spread of the strong reflections from each crystal plane. Accordingly, the deformation mechanism of st-PVA films was confirmed to be essential equal to that of at-PVA one. Anyway, we must emphasize again that the deformation mechanism of at- and st-PVA films is quite different from ultradrawing mechanisms of polyethylene associated with a significant crystal transformation from a folded to a fibrous structure [15–17].

It should be noted that at-PVA has advantage in producing high-strength and high-modulus fibers and/or films in comparison with st-PVA. However, the crystallinity lower than 50% of drawn PVA films is a serious problem to produce an ideal sample whose Young's modulus is close to the crystal lattice modulus [20, 21]. Namely, a drastic increase in crystallinity under elongation must be taken into consideration. If this can be realized, PVA films (or fibers) have the possibility of successfully increasing of Young's modulus. Because of high stereo-regularity, the possibility of successfully increasing in crystallinity may be better for st-PVA than for at-PVA, although the greatest significant drawability of st-PVA films, at present, is a little bit lower than that of at-PVA one.

Conclusion

The drawability of at- and st-PVA films has been studied as a function of composition of mixed solvent and the temperature of gelation/crystallization. Through a series of experiments, it was found that the maximum draw ratio could be realized when the gels were prepared from a solution with 60/40 composition by quenching at −80 °C. Young's modulus and tensile strength of at-PVA films were higher than those of st-PVA ones. This is due to the fact that the values of birefringence measured for drawn

at-PVA films are higher than those of st-PVA films although the corresponding crystallinities are somewhat lower. To check the origin of the significant drawability, the morphological properties of at- and st-PVA undrawn films were studied. The meshy-like fibrillar texture within undrawn films became finer and the corresponding crystallinity became lower with decreasing the temperature of gelation/crystallization. However, the continuous fine meshy tissue of at-PVA film showed no optical anisotropy, while the tissue of the st-PVA film was anisotropic rod-like texture. Furthermore the crystallinity of undrawn at-PVA films was somewhat lower than that of st-PVA film. This means that the continuous fine meshy tissue with no optical anisotropy and with low crystallinity assures the significant drawability of the resultant dry gel films by transmitting inner stress under elongation.

References

1. Hulse G, Kersting RJ, Warful DR (1981) J Polym Sci Polym Phys Ed 19:655
2. Wang CS, Yeh GS (1981) Polym J 13:341
3. Bhateja SK (1983) J Macromol Sci Phys B22(1):159
4. de Boer J, van den Berg H-J, Pemgs AJ (1984) Polymer 25:513
5. Matsuo M, Sawatari C (1986) Macromolecules 19:2028
6. Matsuo M, Sawatari C (1987) Macromolecules 20:1745
7. Yamaura K, Katoh H, Tanigami T, Matsuzawa S (1987) J Appl Polym Sci 34:2345
8. Yamaura K, Itoh M, Tanigami T, Matsuzawa S (1989) J Appl Polym Sci 37:2709
9. Yamaura K, Tanigami T, Hayashi N, Okura S, Takemura Y, Itoh M, Matsuzawa S (1990) J Appl Polym Sci 40:905
10. Sawatari C, Yamamoto Y, Yanagida N, Matsuo M (1993) Polymer 34:956
11. Matsuo M Kawase M, Sugiura Y, Takematsu S, Hara C (1993) Macromolecules 26:4461
12. Cha WI, Hyon SH, Ikeda Y (1994) J Polym Sci Polym Phys Ed 32:297
13. Mori S (1978) J Chromatogr 157:75
14. Sakurada I, Nukushina K, Sone Y (1955) Koubunshi Kagaku 12:506
15. Smith P, Lemstra PJ, Pijpers JPL, Kiel AM (1981) Colloid Polym Sci 258:1070
16. Matsuo M, Inoue K, Abumiya N (1984) Sen-i Gakkaishi 40:275
17. Matsuo M, Sawatari C, Iida M, Yoneda M (1985) Polymer J 17:1197
18. Matsuo M, Tamada M, Terada T, Sawatari C, Niwa M (1982) Macromolecules 15:988
19. Sawatari C, Iida M, Matsuo M (1984) Macromolecules 17:1765
20. Sakurada I, Nukushina Y, Ito T (1962) J Polym Sci 57:651
21. Matsuo M, Harashina Y, Ogita T (1993) Polymer J 25:319